



ORIGINAL ARTICLE

Therapeutic inhibition of polo-like kinases in anaplastic thyroid cancer

Shu-Fu Lin^{1,2,3}  | Chun-Nan Yeh^{3,4} | Yu-Tung Huang⁵  | Ting-Chao Chou⁶ | Richard J. Wong⁷ 

¹Department of Internal Medicine, New Taipei Municipal TuCheng Hospital, New Taipei City, Taiwan

²Department of Internal Medicine, Chang Gung Memorial Hospital, Taoyuan, Taiwan

³College of Medicine, Chang Gung University, Taoyuan, Taiwan

⁴Department of Surgery, Chang Gung Memorial Hospital, Taoyuan, Taiwan

⁵Center for Big Data Analytics and Statistics, Chang Gung Memorial Hospital, Taoyuan, Taiwan

⁶Laboratory of Preclinical Pharmacology Core, Memorial Sloan-Kettering Cancer Center, New York, NY, USA

⁷Head and Neck Service, Department of Surgery, Memorial Sloan-Kettering Cancer Center, New York, NY, USA

Correspondence

Shu-Fu Lin, Department of Internal Medicine, New Taipei Municipal TuCheng Hospital, New Taipei City, Taiwan.
Email: mmg@cgmh.org.tw

Present address

Ting-Chao Chou, PD Science, Inc., Paramus, NJ, USA

Funding information

Chang Gung Memorial Hospital, Linkou, Grant/Award Number: CMRPG3H0201 and CMRPG3E0353; National Institutes of Health, Grant/Award Number: P30 CA008748

Abstract

Polo-like kinases (PLKs) are potent regulators of cell proliferation and cell survival. Polo-like kinases are potential targets in the treatment of anaplastic thyroid cancer (ATC), a rare but deadly disease. The therapeutic effects of volasertib, a PLK inhibitor, was evaluated for the treatment of ATC either alone or in combination with sorafenib. Volasertib decreased cell viability in three ATC cell lines (8505C, 8305C, and KAT18) in a dose-dependent manner. Volasertib caused ATC cells to accumulate in G₂/M phase, activated caspase-3 activity, and induced apoptosis. Combination therapy using volasertib and sorafenib in ATC cells showed mostly synergistic effects. In vivo studies revealed that combination therapy of volasertib and sorafenib was effective in the treatment of 8505C xenografts. Single-agent volasertib treatment was sufficient to retard 8305C tumor growth. No substantial morbidity was observed in animals that received either single-agent or combination treatment. These preclinical findings suggest that volasertib could be an effective drug in treating ATC.

KEYWORDS

anaplastic thyroid cancer, combination therapy, polo-like kinase, sorafenib, volasertib

Abbreviations: ATC, anaplastic thyroid cancer; CI, combination index; OD, optical density; PCNA, proliferating cell nuclear antigen; PI, propidium iodide; PLK, polo-like kinase.

This is an open access article under the terms of the Creative Commons Attribution-NonCommercial License, which permits use, distribution and reproduction in any medium, provided the original work is properly cited and is not used for commercial purposes.

© 2020 The Authors. Cancer Science published by John Wiley & Sons Australia, Ltd on behalf of Japanese Cancer Association.

1 | INTRODUCTION

Anaplastic thyroid cancer is a rare disease, and one of the most aggressive malignancies. Anaplastic thyroid cancer represents less than 1% of all thyroid cancers, but is responsible for 14%–39% of thyroid cancer mortality. The disease is typically fatal, with a dismal median survival of only 3–5 months, and 1-year mortality of 80%.^{1–4} Recently, the US FDA approved a BRAF inhibitor (dabrafenib) plus a MEK inhibitor (trametinib) for locally advanced, metastatic ATC with BRAF V600E mutation. However, approximately half of patients with ATC lack this mutation, rendering them insensitive to this approach. In addition, most patients with the BRAF V600E mutation will acquire resistant disease or discontinue treatment due to adverse effects of dabrafenib and trametinib.⁵ Therefore, there is an urgent need for the discovery of new treatments with different mechanisms of action for patients with ATC.

The PLK family is a group of five serine/threonine kinases (PLK1–5) that regulates multiple biological functions.^{6–8} Polo-like kinase 1 is a well-established member of the PLK family; it participates in G₂/M transition, centrosome maturation, spindle assembly, mitosis, cytokinesis, DNA damage repair, and apoptosis.^{6–11} Both PLK2 and PLK4 are required for centrosome duplication during the cell cycle.^{12,13} Polo-like kinase 3 is a stress response protein that is activated in response to a variety of stress conditions, including DNA damage, mitotic, oxidative, and hypoxic stress.¹⁴ Polo-like kinase 5 is primarily expressed in the brain and has a glioblastoma suppressor function.¹⁵ Because of their critical roles in cell proliferation and cell survival, PLKs are considered to be attractive targets for cancer therapy.⁸ Polo-like kinase 1 has been reported to be a therapeutic target in preclinical models of ATC.^{16–18}

Volasertib (BI 6727) is a highly selective and potent inhibitor of PLK1, PLK2, and PLK3, with 50% enzyme inhibitory concentrations at low nanomolar concentrations (0.87, 5, and 56 nmol/L, respectively).¹⁹ Volasertib has been shown to induce G₂/M arrest, activate caspase-3, and induce apoptotic cell death in leukemia cells.²⁰ Treatment with volasertib reveals adequate tumor tissue penetration, efficacy in treating animal models of malignancy (colon, leukemia, and lymphoma), and favorable safety profiles.^{19–21} Volasertib has shown therapeutic effects against ovarian cancer in a phase II trial.²² In this study, we report the results of the effects of volasertib alone and in combination with sorafenib, a multikinase inhibitor approved for the treatment of differentiated thyroid cancer²³ and ATC.

2 | MATERIALS AND METHODS

2.1 | Anaplastic thyroid cancer cell lines

Three human ATC cell lines, 8505C, 8305C, and KAT18, were evaluated in this study.^{24–26} Cell line identity was validated using DNA short tandem repeat profiling and cells were stored in liquid nitrogen until use. 8505C and 8305C cell lines were maintained in MEM

culture medium with sodium pyruvate (1 mmol/L) and sodium bicarbonate (2.2 g/L). The KAT18 cell line was maintained in RPMI-1640 medium with sodium bicarbonate (2.0 g/L). Both MEM and RPMI-1640 were supplemented with 10% FCS, 100 000 units/L penicillin, and 100 mg/L streptomycin. These ATC cell lines were incubated in a humidified incubator with 5% CO₂ at 37°C.

2.2 | Drugs

Volasertib and sorafenib were obtained from Selleck Chemicals. For in vitro experiments, volasertib and sorafenib were prepared using DMSO (Sigma) to a stock concentration of 10 mmol/L and stored at –80°C until further use. For in vivo experiments, volasertib was formulated at a concentration of 4.3 mg/mL in poly(ethylene glycol) 300 (Sigma) and distilled water (2:3 v/v) and stored at –80°C. Sorafenib was formulated at a concentration of 57.6 mg/mL in 50% Kolliphor EL (Sigma) and 50% ethanol (Sigma) and stored at –80°C; it was further dissolved at a final concentration of 14.4 mg/mL in water before in vivo use.

2.3 | Antibodies

Primary Abs against PLK1, PLK2, PLK3, cleaved caspase-3, p-Histone H3 (Ser10), PCNA, and β-actin were acquired from Cell Signaling Technology. Alpha-tubulin Ab was purchased from Sigma.

2.4 | Cell viability assays and drug combination studies

Cells were seeded at 2×10^3 cells (8505C), 2×10^4 cells (8305C), and 1×10^4 cells (KAT18) per well in 24-well plates in 1 mL media and were incubated overnight. The ATC cells were then exposed to six serial two-fold dilutions of volasertib, sorafenib, or placebo over a 4-day treatment course. Cell viability was assessed by the CytoTox 96 kit (Promega) using a spectrophotometry (Infinite M200 PRO; Tecan). CompuSyn software was applied to determine the IC₅₀ values of volasertib and sorafenib for each cell line on day 4.^{27,28}

To study combination therapy with volasertib and sorafenib, ATC cells were seeded as described above and were incubated overnight. Cells were exposed to vehicle, volasertib, sorafenib, or combination therapy of volasertib and sorafenib for a 4-day treatment. Six consecutive two-fold dilutions were evaluated from the following beginning doses for 8505C, 8305C, and KAT18, respectively: volasertib at 90.8, 140.8, and 204.8 nmol/L and sorafenib at 34.0, 26.4, and 35.6 μmol/L. These doses selected were based on the IC₅₀ of each drug in 8505C, 8305C, and KAT18 cell lines determined in this study. Drug combination effects were evaluated by computing the CI using the Chou-Talalay method and CompuSyn software.^{27,28} The CI was used to quantitatively determine for synergism (CI < 1), additive effect (CI = 1), and antagonism (CI > 1) in drug combinations.

2.5 | Western blot analysis

Anaplastic thyroid cancer cells were treated with volasertib (100 nmol/L) or vehicle for the indicated periods after seeding the cells at 1×10^6 cells in 100-mm petri dishes in 10 mL media overnight. Cell pellets were collected and dissolved using an immunoprecipitation assay buffer containing protease and phosphatase inhibitor mixture, which were then clarified by centrifugation. Protein lysate (40 μ g) was separated on 12% Tris-HCl gels and transferred to PVDF membranes. The membranes were blocked with 5% non-fat milk and incubated with primary Ab at 4°C overnight, followed by a HRP-conjugated secondary Ab. A chemiluminescence reagent (PerkinElmer) was used to detect signals. The ratios of basal PLK1, PLK2, and PLK3 to β -actin for each cell line were calculated. Relative expression was analyzed using the 8505C value as reference.

Tumor levels of PLK1, PLK2, PLK3, PCNA, and cleaved caspase-3 were evaluated in mice treated with placebo, volasertib, sorafenib, or combination therapy by western blot analysis. At indicated periods, animals were killed with carbon dioxide, the tumors were harvested, mixed with protein extraction buffer (GE Healthcare), homogenized, and sonicated on ice. After centrifugation, clarified supernatants were aliquoted and stored at -80°C for immunoblotting as described above.

2.6 | Cell cycle analyses

To evaluate the effect of volasertib on cell cycle progression, ATC cells were seeded overnight at 4×10^5 cells per well in 6-well plates in 2 mL media. Vehicle or volasertib (100 nmol/L) was added and the cells were incubated for 24 hours. Adherent cells were then collected, washed with PBS, fixed with 70% ethanol at 4°C, and stained DNA using DNA staining solution containing RNase A (100 μ g/mL; Sigma) and PI (5 μ g/mL; Sigma) at 37°C for 15 minutes. Data were acquired using flow cytometry (BD FACSCalibur Flow Cytometer; BD Biosciences).

2.7 | Apoptosis detection

A fluorometric assay kit (Abcam) was used to measure caspase-3 activity. After plating cells at 1×10^6 cells in 100-mm petri dishes in 10 mL media overnight, vehicle or volasertib (100 nmol/L) was added and incubated for 24 hours. Adherent cells (5×10^5) were collected, lysed, and incubated with caspase-3 substrate (DEVD-AFC) and reaction mixture at 37°C for 1.5 hours. A spectrophotometer (Infinite M200 PRO; Tecan) was used to detect caspase-3 activity.

We measured early apoptosis by staining cells with annexin V-Alexa Fluor 488 and PI (Invitrogen). Anaplastic thyroid cancer cells were seeded in 6-well plates in 2 mL media at a density of 4×10^5 cells overnight and then treated with vehicle or volasertib (100 nmol/L) for 24 hours. Following the manufacturer's protocol, adherent cells were collected, washed with PBS, and incubated with

annexin V-Alexa Fluor 488 and PI at room temperature for 15 minutes in the dark. Flow cytometry (BD FACSCalibur Flow Cytometer; BD Biosciences) was used to detect early apoptotic cells (annexin V-positive, PI-negative).

Induction of sub- G_1 apoptotic cells by volasertib treatment was assessed using flow cytometry. Anaplastic thyroid cancer cells were plated in 6-well plates in 2 mL media at a density of 4×10^5 cells overnight, and treated with vehicle or volasertib (100 nmol/L) for 24 hours. Floating cells and trypsinized adherent cells were collected, and samples were prepared as described earlier for cell cycle analyses. Flow cytometry (BD FACSCalibur Flow Cytometer; BD Biosciences) was used to detect apoptotic sub- G_1 cells. Induction of sub- G_1 apoptotic cells in 8505C, 8305C, and KAT18 cells treated with placebo, volasertib (22.7, 35.2, and 102.4 nmol/L, respectively), sorafenib (8.5, 35.2, and 17.8 μ mol/L, respectively), and in combination was assessed after a 48-hour treatment.

2.8 | Immunofluorescence microscopy

We used confocal microscopy to evaluate the effect of volasertib on mitosis. After plating ATC cells at 5×10^4 cells in 4-well culture slides in 1 mL media overnight, vehicle or volasertib (100 nmol/L) was added and incubated for 24 hours. The cells were then fixed in 4% paraformaldehyde (Sigma), washed with PBS, permeabilized with 0.1% Triton X-100 for 10 minutes at room temperature, and washed with PBS. The cells were incubated at 4°C overnight with primary rabbit p-Histone H3 (Ser10) Ab and mouse α -tubulin Ab. The cells were then washed with PBS, incubated for 25 minutes at 37°C with secondary Alexa Fluor 633-conjugated goat anti-rabbit Ab (Invitrogen) and Alexa Fluor 488-conjugated goat anti-mouse Ab (Life Technologies), washed with PBS, incubated for 10 minutes at room temperature with DAPI (Invitrogen). Chromosomes were examined to identify mitotic cells. Leica TCS SP8 X confocal microscopy (Leica Microsystems) was used to capture images.

The expression of cleaved caspase-3 (active form of caspase-3) was evaluated by immunofluorescence microscopy. Anaplastic thyroid cancer cells were seeded at 5×10^4 cells in 4-well culture slides in 1 mL media overnight. Vehicle or volasertib (100 nmol/L) was added and incubated for 24 hours; the cell samples were then prepared as described in mitosis assessment. Next, the cells were incubated at 4°C overnight with primary rabbit cleaved caspase-3 Ab and mouse α -tubulin Ab. The cells were then incubated for 25 minutes at 37°C with secondary Alexa Fluor 633-conjugated goat anti-rabbit Ab and Alexa Fluor 488-conjugated goat anti-mouse Ab. Leica TCS SP8 X confocal microscopy (Leica Microsystems) was used to capture images.

2.9 | In vivo flank tumor therapy

Female athymic nude mice aged 7-10 weeks were obtained from the National Laboratory Animal Center, Taiwan. Mice were

inoculated with 1×10^6 cells (1:1 Matrigel : culture medium) into the s.c. flanks for 8505C and 8305C models. 8505C and 8305C cell lines were chosen because they possess promising tumorigenesis rates.

Mice bearing 8505C and 8305C tumors received placebo, volasertib (25 mg/kg, 2 days on and 5 days off, once a day), sorafenib (40 mg/kg, 4 days on and 3 days off, once a day), or combination treatment for three cycles of therapy. The doses of volasertib and sorafenib chosen were based on previous reports.^{19,29} Tumor volume and body weight of each animal were measured twice a week.

This study protocol was approved by the Chang Gung Memorial Hospital's Committee of Laboratory Animal Center at Linkou (No. 2013121401).

2.10 | Statistical analyses

SPSS software (version 25; IBM) was used for statistical analyses. Student's *t* test was used for in vitro studies where two independent groups were compared. One-way ANOVA with post-hoc Scheffe test was used for in vivo experiments to compare more than two group means. Pearson's correlation coefficient was used to determine the association between IC_{50} of volasertib and basal PLK expression. Results are expressed as mean \pm SE. Statistically significant was considered when *P* was less than .05.

3 | RESULTS

3.1 | Volasertib induces cytotoxicity in ATC cell lines

Volasertib decreased cell survival in three ATC cell lines in a dose-dependent fashion (Figure 1A). Volasertib at 100 nmol/L arrested cell growth by 90.5% (8505C), 88.9% (8305C), and 80.3% (KAT18) on day 4. The cytotoxicity of volasertib in these ATC cell lines was assessed by CompuSyn software. The IC_{50} was calculated on day 4 (Figure 1B). 8505C cells had the lowest IC_{50} (22.7 ± 0.1 nmol/L) and KAT18 cells had the highest IC_{50} (51.2 ± 0.9 nmol/L). These median-effective doses of volasertib in ATC cells are much lower than the achievable serum concentration (551.1 nmol/L) reported in a recent clinical trial.²²

3.2 | Volasertib modulates the expression of PLKs

Volasertib has been shown to increase the level of PLK1 in HeLa cells.³⁰ The effects of volasertib (100 nmol/L) on PLK1 expression was assessed in three ATC cell lines (Figure 1C). Volasertib treatment significantly induced PLK1 levels by 4 hours (8505C), 16 hours (8305C), and 8 hours (KAT18). In addition, volasertib treatment decreased PLK2 expression by 24 hours (8505C and 8305C) and 4 hours (KAT18). Expression of PLK3 was not significantly altered by volasertib treatment in 8505C, 8305C, or KAT18 cells during a 24-hour treatment.

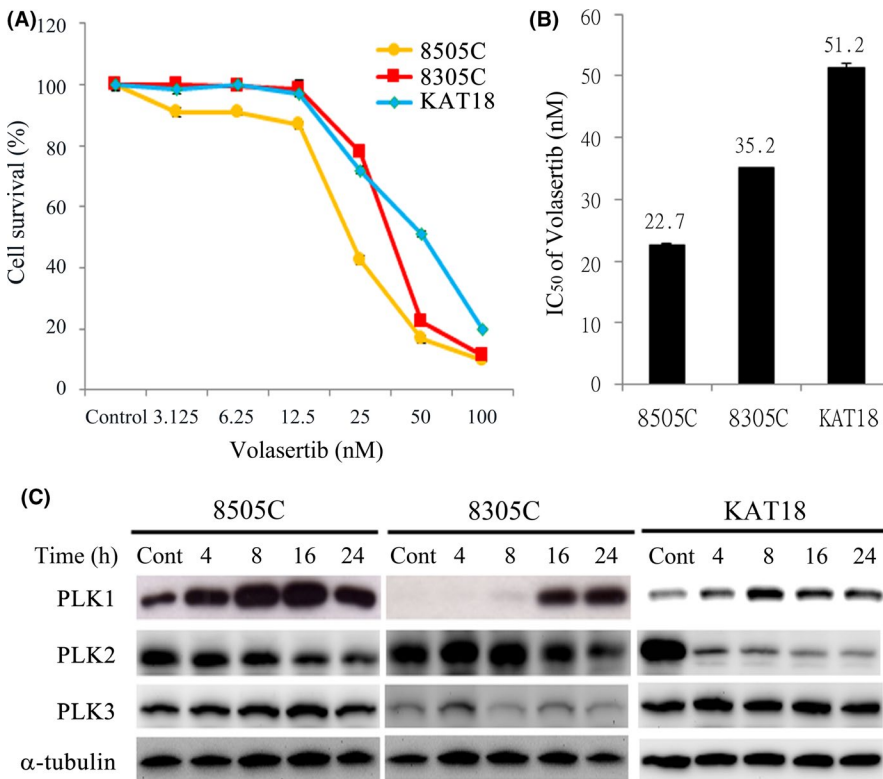


FIGURE 1 Volasertib induces cytotoxicity and alters polo-like kinase (PLK) expression in three anaplastic thyroid cancer (ATC) cell lines. A, Cytotoxicity was evaluated in 8505C, 8305C, and KAT18 cells treated with a series of six two-fold dilutions of volasertib starting from 100 nmol/L. Dose-response curves were obtained on day 4 using lactate dehydrogenase assays. B, The IC_{50} of volasertib on day 4 was calculated for three ATC cell lines using CompuSyn software. C, The expression of PLK1, PLK2, and PLK3 was evaluated by western blotting in 8505C, 8305C, and KAT18 cells treated with volasertib (100 nmol/L) or placebo for the indicated periods. Cont, control

3.3 | Volasertib affects cell cycle progression

We evaluated the effect of volasertib (100 nmol/L for 24 hours) on cell cycle distribution in three ATC cell lines, and compared these data with untreated control cells. The represented cell line 8505C is shown in Figure 2A. Volasertib treatment significantly increased cell accumulation in G2/M phase in 8505C ($82.6 \pm 0.2\%$ and $12.2 \pm 0.0\%$, $P < .001$), 8305C ($83.4 \pm 0.2\%$ and $24.6 \pm 0.2\%$, $P < .001$), and KAT18 ($32.7 \pm 0.4\%$ and $9.9 \pm 0.4\%$, $P < .001$; Figure 2B).

Confocal microscopy was used to assess the ability of volasertib (100 nmol/L for 24 hours) to block ATC cells in mitosis (Figure 2C). Mitotic cells were recognized, and the mitotic index was analyzed for three ATC cell lines (Figure 2D). Compared to the control group, volasertib treatment substantially increased the proportion of mitotic cells in the 8505C ($6.7 \pm 0.3\%$ and $1.6 \pm 0.1\%$, $P < .001$), 8305C ($22.0 \pm 1.9\%$ and $0.8 \pm 0.2\%$, $P < .001$), and KAT18 ($3.9 \pm 0.5\%$ and $1.2 \pm 0.2\%$, $P = .002$) cell lines.

Based on chromosomal features, mitosis consists of prophase, prometaphase, metaphase, anaphase, and telophase.³¹ The distribution of cells in mitosis was evaluated. Statistical analyses indicated the proportions of prometaphase cells were significantly increased by volasertib (100 nmol/L for 24 hours) in 8505C ($74.1 \pm 1.6\%$ and $45.9 \pm 1.6\%$, $P < .001$), 8305C ($91.4 \pm 2.5\%$ and $51.7 \pm 1.5\%$, $P < .001$), and KAT18 cells ($70.0 \pm 4.9\%$ and $43.0 \pm 3.3\%$, $P < .001$) compared to control therapy (Figure 2E). This finding of mitotic arrest in prometaphase represents a typical phenotype of PLK arrest.³²

3.4 | Volasertib treatment induces apoptotic cell death in ATC cells

Induction of apoptosis is a frequent mechanism of activity by cancer therapeutics.³³ A prior report revealed that volasertib treatment increased caspase-3 activity and led to apoptosis in lymphoma cells.²¹ The ability of volasertib (100 nmol/L) to activate caspase-3 activity in 8505C, 8305C, and KAT18 cells was evaluated by a fluorometric assay kit after 24 hours of treatment (Figure 3A). Caspase-3 activity was significantly increased by volasertib compared to control treatment in 8505C (0.032 ± 0.000 -OD and 0.011 ± 0.000 -OD, $P < .001$), 8305C (0.026 ± 0.000 -OD and 0.013 ± 0.000 -OD, $P = .002$), and KAT18 cells (0.098 ± 0.001 -OD and 0.082 ± 0.001 -OD, $P = .004$), revealing activation of caspase-3. The expression of cleaved caspase-3 was assessed using immunofluorescence staining to confirm volasertib treatment led to caspase-3 activation in ATC cells. The expression of cleaved caspase-3 in 8505C cells is shown in Figure 3B. The proportions of ATC cells with cleaved caspase-3 staining were analyzed (Figure 3C). Volasertib treatment at 100 nmol/L for 24 hours significantly induced more cells with cleaved caspase-3 staining in 8505C ($8.9 \pm 2.3\%$ and $1.1 \pm 0.5\%$, $P = .003$), 8305C ($6.8 \pm 1.5\%$ and $1.6 \pm 0.6\%$, $P = .010$), and KAT18 cells ($1.9 \pm 0.4\%$ and $0.2 \pm 0.1\%$, $P = .002$) compared with placebo treatment.

Stimulation of caspase-3 activity could result in apoptosis. The ability of volasertib to induce early apoptosis was determined using

annexin V-Alexa Fluor 488 and PI staining (Figure 3D). Statistical analyses show volasertib (100 nmol/L for 24 hours) significantly increased early apoptotic cells in 8505C ($4.0 \pm 0.1\%$ and $1.9 \pm 0.0\%$, $P < .001$), 8305C ($4.0 \pm 0.2\%$ and $2.3 \pm 0.3\%$, $P = .002$), and KAT18 cells ($11.3 \pm 0.2\%$ and $0.4 \pm 0.0\%$, $P < .001$) when compared with placebo treatment (Figure 3E).

8505C, 8305C, and KAT18 cells were incubated with volasertib at 100 nmol/L for 24 hours. The capacity of volasertib to induce sub-G₁ apoptosis in these ATC cell lines was assessed (Figure 3F). Statistical analyses revealed that volasertib significantly induced a greater proportion of sub-G₁ cells in 8505C ($9.2 \pm 0.1\%$ and $3.2 \pm 0.2\%$, $P < .001$), 8305C ($4.1 \pm 0.2\%$ and $2.9 \pm 0.1\%$, $P = .006$), and KAT18 cells ($37.6 \pm 0.1\%$ and $8.8 \pm 0.2\%$, $P < .001$) compared with controls (Figure 3G). These results indicate that volasertib treatment induces apoptotic cell death in ATC cells.

3.5 | Synergism of volasertib and sorafenib in ATC cells

Sorafenib as single-agent therapy has only a mild effect in patients with advanced ATC,³⁴ with a limited response rate (15%) and no impact on median survival (3.9 months). Approaches to enhance the efficacy of sorafenib therapy would have clinical value. We assessed the effects of applying volasertib combined with sorafenib in three ATC cell lines.

The therapeutic effects of sorafenib in 8505C, 8305C, and KAT18 cell lines were assessed after a 4-day treatment course (data not shown). On day 4, the IC₅₀ of sorafenib was 8.5 μ mol/L in 8505C, 6.6 μ mol/L in 8305C, and 8.9 μ mol/L in KAT18 cells as calculated using CompuSyn software.

Combination therapeutic effects of volasertib and sorafenib were studied (Figure 4A). In 8505C, 8305C, and KAT18 cells, combination therapy with volasertib and sorafenib had increased cytotoxicity compared to either therapy alone. The CI of volasertib and sorafenib was evaluated using the Chou-Talalay method. The combination of volasertib and sorafenib spanned from synergistic to antagonist effects in 8505C (CI, 0.84-1.11), 8305C (CI, 0.89-1.07), and KAT18 cells (CI, 0.78-1.11; Figure 4B). The combination of volasertib and sorafenib was synergistic when higher percentages of cells were affected in 8505C (fraction affected 0.2 or higher), 8305C (fraction affected 0.3 or higher), and KAT18 cells (fraction affected 0.2 or higher).

Prior reports reveal that both volasertib and sorafenib have the ability to induce apoptotic cell death.^{21,35} We sought to determine whether the combination of volasertib and sorafenib could lead to higher proportions of sub-G₁ apoptotic cells than single-agent and placebo therapy in 8505C, 8305C, and KAT18 cell lines (Figure 4C). Volasertib and sorafenib combination therapy significantly induced more sub-G₁ cells than volasertib, sorafenib, or control treatment in three ATC cell lines, suggesting apoptosis is one of the mechanisms contributing to improved therapeutic effect of combination therapy over single-agent therapy in ATC cells.

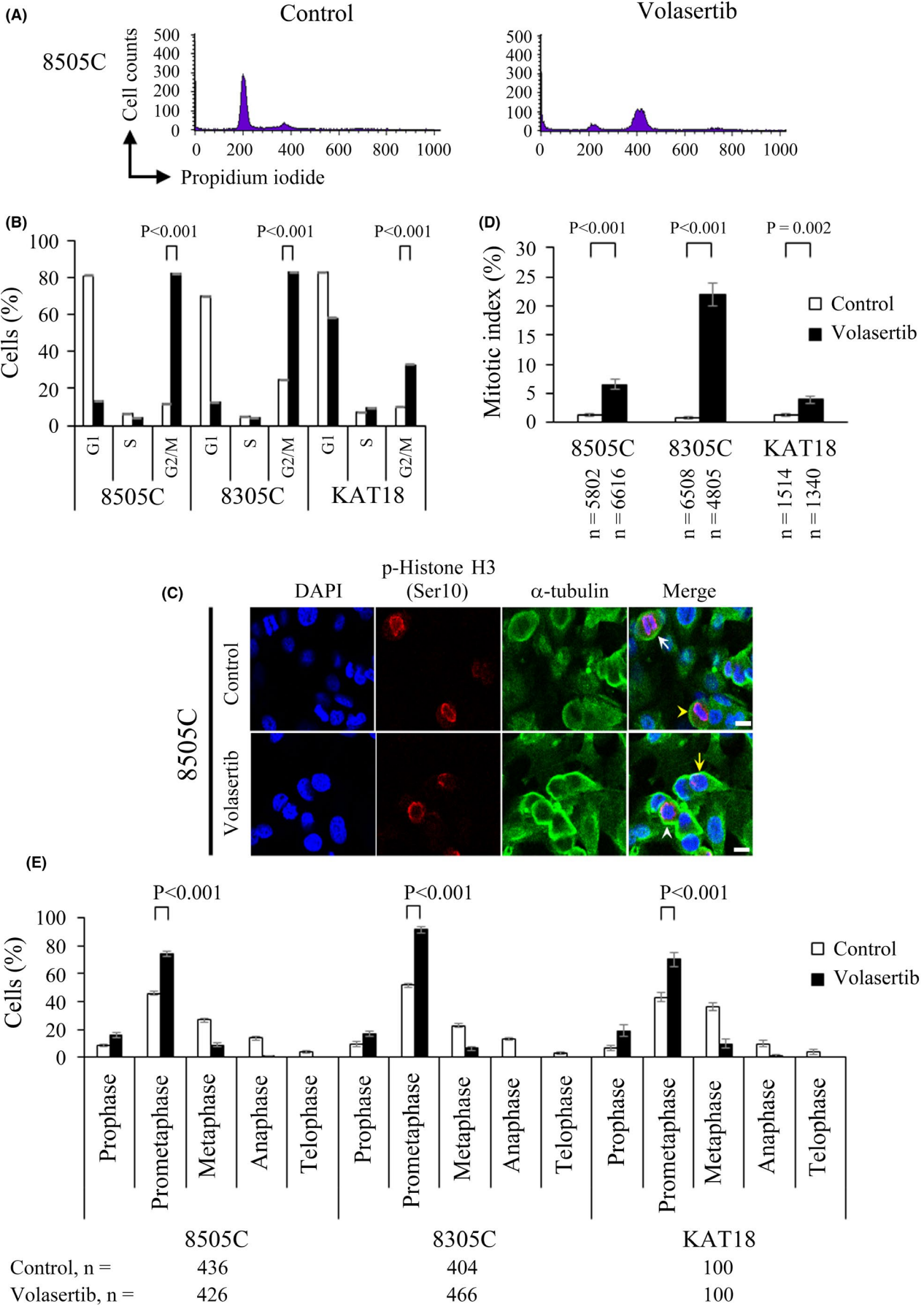


FIGURE 2 Volasertib accumulates cells in G₂/M phase and inhibits mitotic progression in prometaphase in anaplastic thyroid cancer (ATC) cells. A, Cell cycle analysis using flow cytometry was performed to evaluate DNA content in 8505C cells treated with placebo or volasertib (100 nmol/L) for 24 h. B, Statistical analyses reveal volasertib (100 nmol/L) treatment for 24 h significantly accumulated cells in G₂/M phase in three ATC cell lines. C, 8505C cells were treated with volasertib (100 nmol/L) or placebo for 24 h and stained with fluorescent Abs against DAPI (blue), p-Histone H3 (Ser10) (red), and α -tubulin (green). Chromosomal appearance was evaluated using immunofluorescence confocal microscopy. Cells in prophase (yellow arrow), prometaphase (white arrowhead), metaphase (yellow arrowhead), and anaphase (white arrow) were identified. D, The proportion of ATC cells in mitosis was assessed after treatment with volasertib (100 nmol/L) or placebo for 24 h. Cells were stained with DAPI, and chromosome characteristics were evaluated using immunofluorescence confocal microscopy. The mitotic index was assessed with a minimum of 1340 cells counted from at least 13 different fields for each condition. Volasertib significantly increased the proportion of 8505C, 8305C, and KAT18 cells in mitosis. E, The distribution of cells in mitosis was determined by counting with a minimal of 100 mitotic cells from at least 10 different fields by confocal microscopy for each condition. Quantification analyses revealed mitotic cells were arrested in prometaphase by the treatment of volasertib (100 nmol/L) for 24 h. Scale bar, 10 μ m

3.6 | Volasertib and sorafenib combination therapy for ATC xenografts

The effects of volasertib and sorafenib combination therapy *in vivo* were evaluated in mice bearing 8505C and 8305C tumors. Nude mice with 8505C flank tumors with a mean diameter of 5.2 mm were treated with oral gavage of placebo, volasertib, sorafenib, or combination therapy ($n = 6$ per group) daily for three cycles (Figure 5A). Single-agent therapy using volasertib or sorafenib did not significantly retard 8505C tumor growth compared with control treatment. However, combination therapy significantly inhibited 8505C tumor growth on day 3 compared to the placebo treatment (1.1 ± 0.0 -fold and 1.7 ± 0.2 -fold, $P = .008$) and this inhibitory efficacy of combination therapy continued until day 20 (1.7 ± 0.3 -fold and 6.1 ± 1.8 -fold, $P = .032$). No substantial reduction in body weight was observed in volasertib, sorafenib, or combination therapy compared to control treatment when the study was closed (Figure 5B). Representative mice bearing 8505C tumors on day 17 are shown in Figure 5C.

Mice bearing 8305C xenografts with a mean diameter of 4.6 mm were treated with oral placebo, volasertib, sorafenib, or combination therapy as described above for 8305C xenografts ($n = 3$ per group; Figure 5D). Volasertib, sorafenib, and combination therapy significantly inhibited 8305C tumor growth by day 10 when compared with control (1.3 ± 0.1 -fold, 2.3 ± 0.7 -fold, 1.0 ± 0.3 -fold, and 9.2 ± 2.4 -fold in volasertib, sorafenib, combination therapy, and the control group, respectively; $P < .05$ for all comparisons), and the therapeutic effects continued through to day 27 (4.1 ± 1.6 -fold, 6.9 ± 4.5 -fold, 1.2 ± 0.5 -fold and 49.4 ± 13.7 -fold, respectively; $P < .05$ for all comparisons). Combination therapy showed similar inhibitory effects in retarding 8305C tumor growth compared with either volasertib or sorafenib monotherapy ($P > .05$ for both comparisons). We did not observe any significant changes in body weight attributable to volasertib, sorafenib, or combination therapy in this study (Figure 5E). Representative mice bearing 8305C tumors were photographed on day 22 (Figure 5F).

The molecular alterations induced by volasertib treatment in 8505C and 8305C xenografts were assessed in mice treated daily with volasertib (25 mg/kg for 2 days; Figure 5G). In 8505C xenografts, volasertib treatment did not significantly change the levels of PLK1, PLK3, or cleaved caspase-3. Polo-like kinase 2 levels were decreased on days 2 and 3. A marker of cell proliferation,³⁶ PCNA, was transiently decreased on day 2. In 8305C tumors, PLK1 expression was increased at

days 2 and 3. Polo-like kinase 2 and 3 and PCNA were decreased and cleaved caspase-3 expression was increased by day 3. Day 2 and 3 were chosen in this study because our prior study revealed that volasertib treatment modulates protein expression at these time points.³⁷

The molecular alterations induced by volasertib, sorafenib, and combination treatment in 8505C tumors were assessed (Figure 5H). Compared with control treatment, volasertib and sorafenib monotherapy decreased the expression of PCNA. This inhibitory effect was not observed in tumors treated with combination therapy. However, combination therapy induced the expression of cleaved caspase-3, which was not observed in mice receiving either volasertib or sorafenib treatment. These data suggest apoptosis was likely one of the working mechanisms of combination therapy in the treatment of 8505C tumors.

The basal expression of PLK1, PLK2, and PLK3 was evaluated in three ATC cell lines (Figure 6A). We sought to determine any correlation between the expression of PLKs and volasertib susceptibility in these ATC cell lines. The susceptibility to volasertib was according to the IC₅₀ value. Relationships between IC₅₀ of volasertib and PLK expression were analyzed using Pearson's correlation coefficients (Figure 6B). The levels of PLK1, PLK2, and PLK3 failed to show any significant correlation with volasertib sensitivity in ATC cells.

4 | DISCUSSION

We found that volasertib effectively inhibited cell survival in three ATC cell lines in this study. Single-agent volasertib treatment efficiently inhibited xenograft growth in the 8305C tumor model. The combination of volasertib and sorafenib significantly retarded 8505C tumor growth compared to control tumors. These results suggest a potential clinical utility of volasertib in treating patients with ATC.

A prior study revealed that volasertib treatment led to increased PLK1 expression in cervical cancer HeLa cells.³⁰ Similarly, we observed that volasertib treatment increased PLK1 expression in 8505C, 8305C, and KAT18 cells. The reasons accounting for this phenomenon are unclear. One potential explanation is that PLK1 expression increased to compensate for the reduced activity of PLK1. Mitotic arrest in prometaphase is a typical phenotype of PLK1 inhibition.³² We found that volasertib treatment led to cell accumulation in prometaphase in 8505C, 8305C, and KAT18 cell lines, suggesting

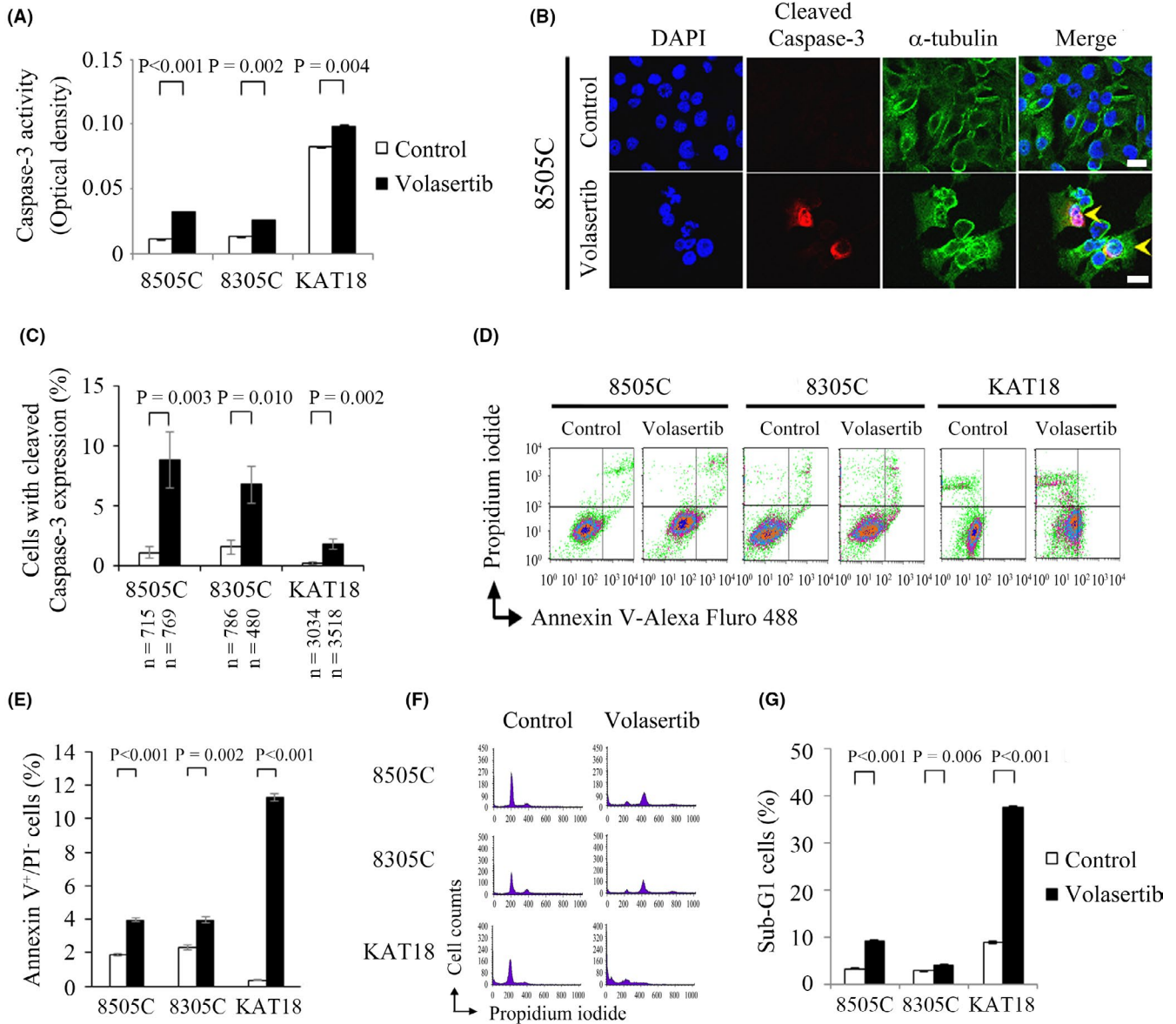


FIGURE 3 Volasertib stimulates caspase-3 activity and induces apoptosis in anaplastic thyroid cancer (ATC) cells. A, Caspase-3 activity was evaluated using a fluorometric assay kit in 8505C, 8305C, and KAT18 cells treated with volasertib (100 nmol/L) or vehicle for 24 h. B, 8505C cells were treated with volasertib (100 nmol/L) or placebo for 24 h and stained with DAPI (blue) and fluorescent Abs against cleaved caspase-3 (red) and α -tubulin (green). Cells with cleaved caspase-3 expression are shown (arrowhead). C, The percentages of ATC cells with cleaved caspase-3 expression were assessed after treatment with placebo or volasertib (100 nmol/L) for 24 h. Cells were stained with fluorescent Abs against cleaved caspase-3, and its expression was evaluated using immunofluorescence confocal microscopy. A minimum of 480 cells from at least 10 different fields was counted for each condition. Volasertib significantly increased the proportion of 8505C, 8305C, and KAT18 cells with cleaved caspase-3 expression. D, Early apoptotic cells were determined by flow cytometry to detect annexin V-positive / propidium iodide (PI)-negative staining in 8505C, 8305C, and KAT18 cells treated with volasertib (100 nmol/L) or vehicle for 24 h. E, Early apoptotic cells were determined by flow cytometry to detect Annexin V-positive / PI-negative staining in 8505C, 8305C, and KAT18 cells treated with volasertib (100 nmol/L) or vehicle for 24 h. Volasertib significantly induced early apoptosis in three ATC cell lines. F, Analysis of cells with sub-G₁ apoptosis was undertaken by evaluating the DNA content using flow cytometry in 8505C, 8305C, and KAT18 cells treated with placebo or volasertib (100 nmol/L) for 24 h. G, Sub-G₁ apoptotic cells were detected by measuring the DNA content of 1×10^4 events for each sample using flow cytometry in cells treated with volasertib (100 nmol/L) or vehicle for 24 h. Volasertib increased the proportion of sub-G₁ cells in three ATC cell lines. Scale bar, 20 μ m

that PLK1 activity was inhibited by volasertib despite the increased protein expression detected.

Volasertib inhibited mitotic progression at prometaphase, which might be one of the working mechanisms of volasertib in the

treatment of ATC cells. In addition to mitotic arrest at prometaphase, we discovered that volasertib arrested cells in the G₂ phase in 8505C, 8305C, and KAT18 cell lines. Volasertib increased the proportion of G₂/M phase cells over that of M phase cells, indicating that volasertib

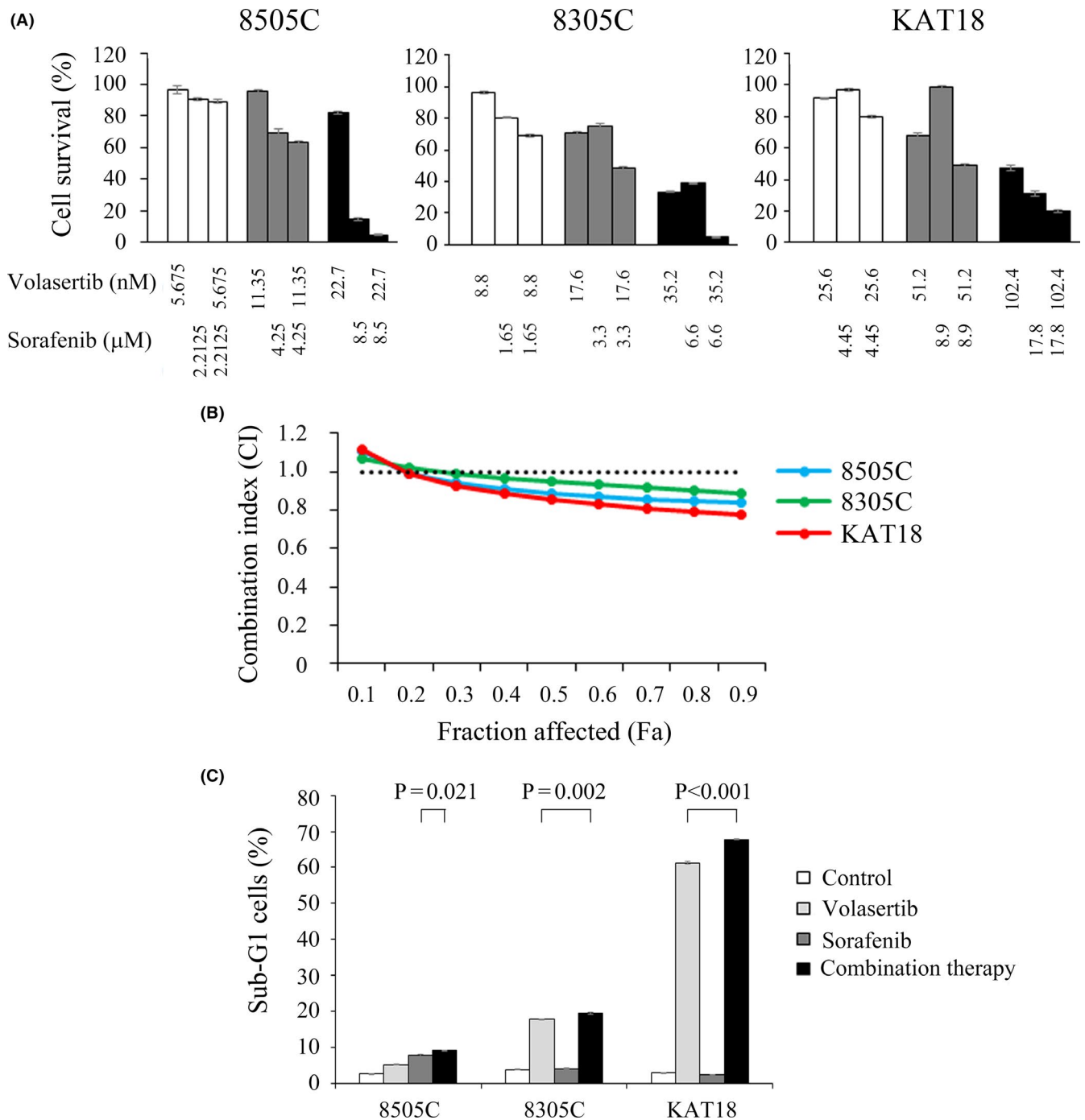
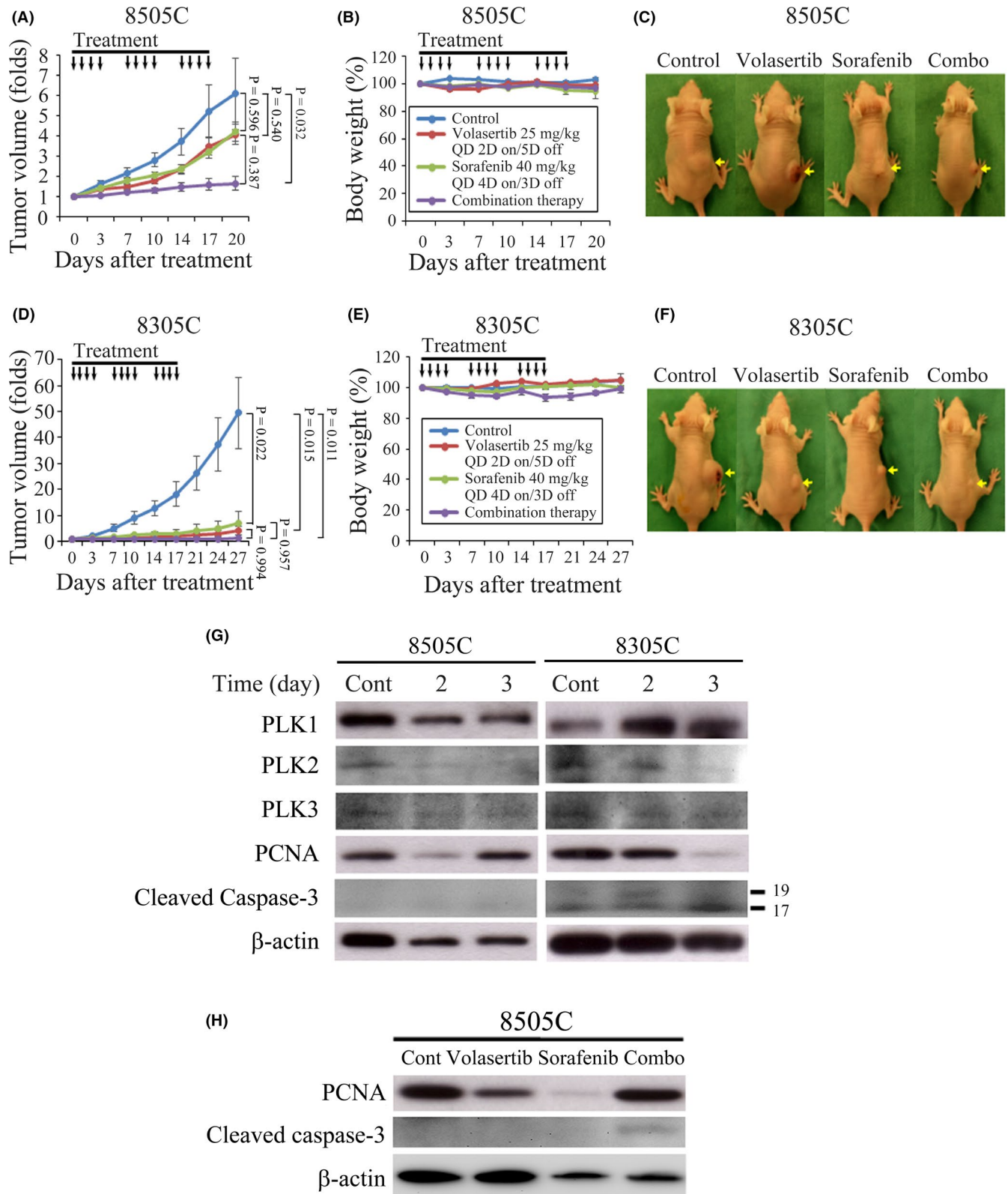


FIGURE 4 Combination therapy of volasertib and sorafenib in anaplastic thyroid cancer (ATC) cells. A, The cytotoxic effects of volasertib and sorafenib alone and in combination after a 4-day treatment in 8505C, 8305C, and KAT18 cells were evaluated using lactate dehydrogenase assays. B, The combination index (CI) of volasertib and sorafenib was calculated using CompuSyn software. Synergistic effects were recognized when higher fractions of cells were affected in 8505C (fraction affected ≥ 0.2), 8305C (fraction affected ≥ 0.3), and KAT18 cell lines (fraction affected ≥ 0.2). The horizontal dotted line at CI = 1 was drawn for discrimination of synergism (CI < 1) and antagonism (CI > 1). C, Analysis of cells with sub-G₁ apoptosis was carried out by evaluating the DNA content using flow cytometry in 8505C, 8305C, and KAT18 cells treated with placebo, volasertib (22.7, 35.2, and 102.4 nmol/L, respectively), and sorafenib (8.5, 35.2, and 17.8 μ mol/L, respectively) alone and in combination for 48 h. Combination therapy significantly increased the proportion of sub-G₁ cells than placebo and single-agent therapy in three ATC cell lines

arrests ATC cells in G₂ phase. Therefore, G₂ phase block is a key mechanism of cytotoxicity in the treatment of ATC cells with volasertib. The inhibition of PLK1 could contribute to G₂ arrest and mitotic block. Polo-like kinase 1 functions start in G₂ and are critical for mitotic entry

and mitotic progression.^{6,38} The effects of PLK1 inhibition might span from a failure at the G₂/M phase transition to mitotic arrest between prophase and anaphase. In this study, volasertib consistently inhibited G₂/M transition and induced mitotic block in the prometaphase in



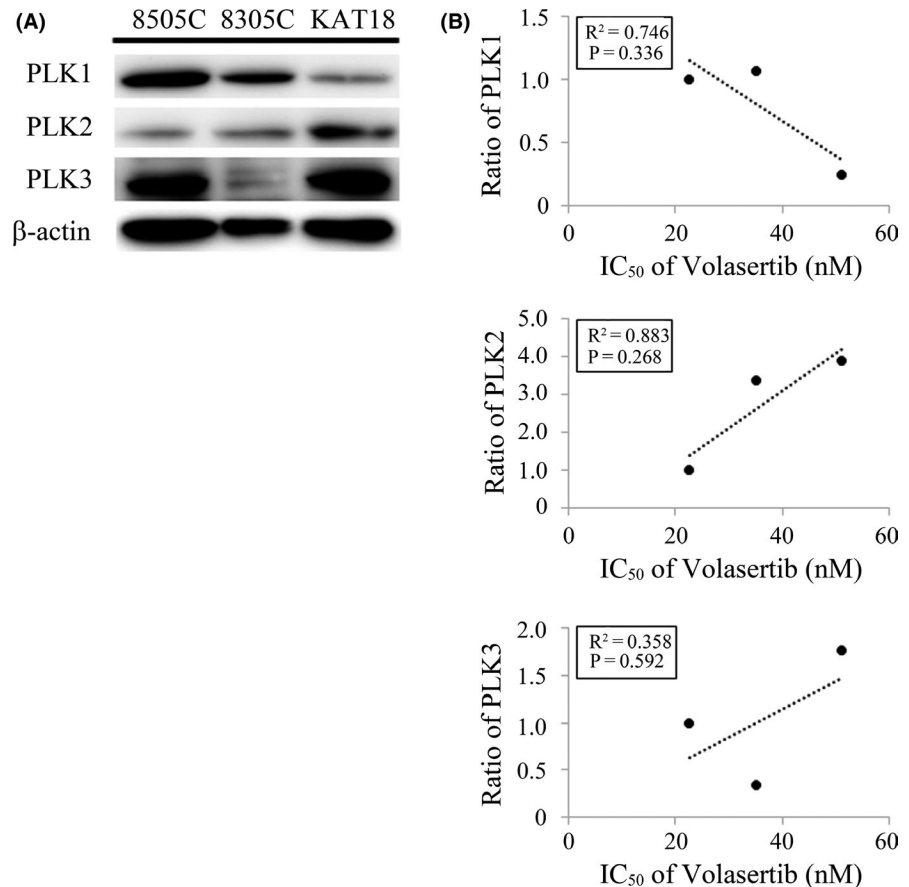
three ATC cell lines. The inhibition of PLK3 has been reported to block mitosis and to arrest cells in G_2/M phase.³⁹

Cancer cells frequently evade apoptosis and the induction of apoptosis is a widely adopted approach of many types of anticancer therapy.³³ Depletion of PLK1 has shown the ability to

induce apoptosis in cancer cells.^{11,38} We found treatment with volasertib activated caspase-3 activity and induced apoptotic cell death in ATC cells. Our data are consistent with prior reports that apoptosis is one of the mechanisms of volasertib for cancer treatment.¹⁹⁻²¹

FIGURE 5 Therapeutic effects of volasertib and sorafenib in murine 8505C and 8305C xenograft tumor models. A, Mice bearing 8505C flank tumors were treated with oral gavage of placebo, volasertib (25 mg/kg, 2 d on and 5 d off), sorafenib (40 mg/kg, 4 d on and 3 d off), or combination therapy daily for three cycles of therapy. Compared with control therapy, volasertib and sorafenib did not significantly retard 8505C tumor growth. However, combination therapy significantly retarded 8505C xenograft growth when compared with control treatment. B, Volasertib, sorafenib, and combination therapy did not significantly decrease body weight compared with control treatment when the study was closed. C, Mice bearing 8505C tumors (yellow arrow) were photographed on day 17. D, Nude mice with established 8305C flank tumors were treated with oral gavage of placebo, volasertib (25 mg/kg, 2 d on and 5 d off), sorafenib (40 mg/kg, 4 d on and 3 d off), or combination therapy daily for three cycles of therapy. Volasertib, sorafenib, and combination therapy significantly inhibited 8305C tumor growth when compared with control mice. E, No substantial decreases in body weight were attributable to volasertib, sorafenib, or combination therapy compared with control treatment. F, Mice bearing 8305C tumors (yellow arrow) were photographed on day 22. G, Tumor levels of polo-like kinase (PLK)1, PLK2, PLK3, proliferating cell nuclear antigen (PCNA), and cleaved caspase-3 were evaluated in 8505C and 8305C xenografts after daily volasertib treatment (25 mg/kg on day 0 and 1) using western blot. H, Tumor levels of PCNA and cleaved caspase-3 were assessed in 8505C xenografts using western blot on day 2 after daily volasertib (25 mg/kg), sorafenib (40 mg/kg) and combination therapy on day 0 and 1. Black arrow, placebo, volasertib, sorafenib, and combination therapy

FIGURE 6 Susceptibility to volasertib and baseline expression of polo-like kinase (PLK)1, PLK2, and PLK3 in anaplastic thyroid cancer (ATC) cell lines. A, Cells were plated at 1×10^6 cells in 100-mm Petri dishes in 10 mL media overnight and cell pellets were collected. Baseline levels of PLK1, PLK2, and PLK3 were evaluated by immunoblot. The sequence of proteins loaded was according to IC_{50} of volasertib. B, Band densities were imaged and quantified using Molecular Imager VersaDoc MP 4000 system (Bio-Rad). Relationships between IC_{50} of volasertib and protein expression were analyzed using Pearson's correlation coefficients, and graphs were drawn using 8505C as reference. The expression of PLK1, PLK2, and PLK3 did not significantly correlate with susceptibility to volasertib in ATC cell lines



Sorafenib therapy has shown some activity in patients with ATC. We examined whether volasertib improved the therapeutic efficacy of sorafenib. Our data reveal promising therapeutic effects of combination therapy of volasertib and sorafenib in the 8505C xenograft model. This combination therapy robustly inhibited 8505C tumor growth compared with control treatment, with promising safety profiles. A recent report reveals the combination of volasertib and a PI3K inhibitor was more effective than either agent alone in the treatment of ATC *in vitro* and *in vivo*.⁴⁰ These findings could broaden the potential clinical application of volasertib in the management of ATC.

In conclusion, volasertib induces cytotoxicity in ATC cells. The therapeutic efficacy of single-agent volasertib was demonstrated in

an 8305C xenograft mouse model. Combination therapy with volasertib and sorafenib showed synergistic effects with higher affected cellular fractions and was highly effective in the treatment of an 8505C xenograft mouse model of ATC. These data support initiation of clinical trials with volasertib alone and in combination with sorafenib in patients afflicted with ATC.

ACKNOWLEDGMENTS

We thank Professor J.-D. Lin and the staff of the Microscope Core Laboratory, the Laboratory Animal Center, and the Expensive Advanced Instrument Core Laboratory of the Chang Gung Memorial Hospital at Linkou for technical support.

CONFLICT OF INTEREST

The authors have no conflict of interest.

ORCID

Shu-Fu Lin  <https://orcid.org/0000-0001-8877-9685>

Yu-Tung Huang  <https://orcid.org/0000-0003-3224-7238>

Richard J. Wong  <https://orcid.org/0000-0001-6259-7314>

REFERENCES

- Kebebew E, Greenspan FS, Clark OH, et al. Anaplastic thyroid carcinoma. Treatment outcome and prognostic factors. *Cancer*. 2005;103:1330-1335.
- Smallridge RC, Ain KB, Asa SL, et al. American Thyroid Association guidelines for management of patients with anaplastic thyroid cancer. *Thyroid*. 2012;22:1104-1139.
- Hsu KT, Yu XM, Audhya AW, et al. Novel approaches in anaplastic thyroid cancer therapy. *Oncologist*. 2014;19:1148-1155.
- Keutgen XM, Sadowski SM, Kebebew E. Management of anaplastic thyroid cancer. *Gland Surg*. 2015;4:44-51.
- Subbiah V, Kreitman RJ, Wainberg ZA, et al. Dabrafenib and trametinib treatment in patients with locally advanced or metastatic BRAF V600-mutant anaplastic thyroid cancer. *J Clin Oncol*. 2018;36:7-13.
- Zitouni S, Nabais C, Jana SC, et al. Polo-like kinases: structural variations lead to multiple functions. *Nat Rev Mol Cell Biol*. 2014;15:433-452.
- de Cárcer G, Manning G, Malumbres M. From Plk1 to Plk5: functional evolution of polo-like kinases. *Cell Cycle*. 2011;10:2255-2262.
- Strebhardt K. Multifaceted polo-like kinases: drug targets and anti-targets for cancer therapy. *Nat Rev Drug Discov*. 2010;9:643-660.
- Yata K, Lloyd J, Maslen S, et al. Plk1 and CK2 act in concert to regulate Rad51 during DNA double strand break repair. *Mol Cell*. 2012;45:371-383.
- Shao C, Chien SJ, Farah E, et al. Plk1 phosphorylation of Numb leads to impaired DNA damage response. *Oncogene*. 2018;37:810-820.
- Liu X, Erikson RL. Polo-like kinase (Plk)1 depletion induces apoptosis in cancer cells. *Proc Natl Acad Sci USA*. 2003;100:5789-5794.
- Cizmecioglu O, Krause A, Bahtz R, et al. Plk2 regulates centriole duplication through phosphorylation-mediated degradation of Fbxw7 (human Cdc4). *J Cell Sci*. 2012;125:981-992.
- Habedanck R, Stierhof YD, Wilkinson CJ, et al. The Polo kinase Plk4 functions in centriole duplication. *Nat Cell Biol*. 2005;7:1140-1146.
- Helmke C, Becker S, Strebhardt K. The role of Plk3 in oncogenesis. *Oncogene*. 2016;35:135-147.
- de Cárcer G, Escobar B, Higuero AM, et al. Plk5, a polo box domain-only protein with specific roles in neuron differentiation and glioblastoma suppression. *Mol Cell Biol*. 2011;31:1225-1239.
- Salvatore G, Nappi TC, Salerno P, et al. A cell proliferation and chromosomal instability signature in anaplastic thyroid carcinoma. *Cancer Res*. 2007;67:10148-10158.
- Nappi TC, Salerno P, Zitzelsberger H, et al. Identification of Polo-like kinase 1 as a potential therapeutic target in anaplastic thyroid carcinoma. *Cancer Res*. 2009;69:1916-1923.
- Russo MA, Kang KS, Di Cristofano A. The PLK1 inhibitor GSK461364A is effective in poorly differentiated and anaplastic thyroid carcinoma cells, independent of the nature of their driver mutations. *Thyroid*. 2013;23:1284-1293.
- Rudolph D, Steegmaier M, Hoffmann M, et al. BI 6727, a Polo-like kinase inhibitor with improved pharmacokinetic profile and broad antitumor activity. *Clin Cancer Res*. 2009;15:3094-3102.
- Rudolph D, Impagnatiello MA, Blaukopf C, et al. Efficacy and mechanism of action of volasertib, a potent and selective inhibitor of Polo-like kinases, in preclinical models of acute myeloid leukemia. *J Pharmacol Exp Ther*. 2015;352:579-589.
- Nguyen T, Parker R, Hawkins E, et al. Synergistic interactions between PLK1 and HDAC inhibitors in non-Hodgkin's lymphoma cells occur in vitro and in vivo and proceed through multiple mechanisms. *Oncotarget*. 2017;8:31478-31493.
- Pujade-Lauraine E, Selle F, Weber B, et al. Volasertib versus chemotherapy in platinum-resistant or -refractory ovarian cancer: a randomized phase II Groupe des Investigateurs Nationaux pour l'Etude des Cancers de l'Ovaire Study. *J Clin Oncol*. 2016;34:706-713.
- Brose MS, Nutting CM, Jarzab B, et al. Sorafenib in radioactive iodine-refractory, locally advanced or metastatic differentiated thyroid cancer: a randomised, double-blind, phase 3 trial. *Lancet*. 2014;384:319-328.
- Ito T, Seyama T, Hayashi Y, et al. Establishment of 2 human thyroid-carcinoma cell-lines (8305c, 8505c) bearing p53 gene-mutations. *Int J Oncol*. 1994;4:583-586.
- Schweppé RE, Klopper JP, Korch C, et al. Deoxyribonucleic acid profiling analysis of 40 human thyroid cancer cell lines reveals cross-contamination resulting in cell line redundancy and misidentification. *J Clin Endocrinol Metab*. 2008;93:4331-4341.
- Lin SF, Lin JD, Hsueh C, et al. Effects of roniciclib in preclinical models of anaplastic thyroid cancer. *Oncotarget*. 2017;8:67990-68000.
- Chou TC. Theoretical basis, experimental design, and computerized simulation of synergism and antagonism in drug combination studies. *Pharmacol Rev*. 2006;58:621-681.
- Chou TC, Martin N. *CompuSyn for Drug Combinations: PC Software and Users Guide: A Computer Program for Quantitation of Synergism and Antagonism in Drug Combinations and the Determination of IC50, ED50, and LD50 Values*. Paramus, NJ, USA: ComboSyn; 2005.
- Kim S, Yazici YD, Calzada G, et al. Sorafenib inhibits the angiogenesis and growth of orthotopic anaplastic thyroid carcinoma xenografts in nude mice. *Mol Cancer Ther*. 2007;6:1785-1792.
- Raab M, Krämer A, Hehlhans S, et al. Mitotic arrest and slippage induced by pharmacological inhibition of Polo-like kinase 1. *Mol Oncol*. 2015;9:140-154.
- Jackson JR, Patrick DR, Dar MM, et al. Targeted anti-mitotic therapies: can we improve on tubulin agents? *Nat Rev Cancer*. 2007;7:107-117.
- Schmucker S, Sumara I. Molecular dynamics of PLK1 during mitosis. *Mol Cell Oncol*. 2014;1:e954507.
- Pfeffer CM, Singh ATK. Apoptosis: a target for anticancer therapy. *Int J Mol Sci*. 2018;19:448.
- Savvides P, Nagaiah G, Lavertu P, et al. Phase II trial of sorafenib in patients with advanced anaplastic carcinoma of the thyroid. *Thyroid*. 2013;23:600-604.
- Garten A, Grohmann T, Kluckova K, et al. Sorafenib-induced apoptosis in hepatocellular carcinoma is reversed by SIRT1. *Int J Mol Sci*. 2019;20:4048.
- Moldovan GL, Pfander B, Jentsch S. PCNA, the maestro of the replication fork. *Cell*. 2007;129:665-679.
- Lin SF, Lin JD, Yeh CN, et al. Targeting PLKs as a therapeutic approach to well-differentiated thyroid cancer. *Endocr Relat Cancer*. 2019;26:727-738.
- Strebhardt K, Ullrich A. Targeting polo-like kinase 1 for cancer therapy. *Nat Rev Cancer*. 2006;6:321-330.
- Wang Q, Xie S, Chen J, et al. Cell cycle arrest and apoptosis induced by human Polo-like kinase 3 is mediated through perturbation of microtubule integrity. *Mol Cell Biol*. 2002;22:3450-3459.
- De Martino D, Yilmaz E, Orlacchio A, et al. PI3K blockage synergizes with PLK1 inhibition preventing endoreduplication and enhancing apoptosis in anaplastic thyroid cancer. *Cancer Lett*. 2018;439:56-65.

How to cite this article: Lin S-F, Yeh C-N, Huang Y-T, Chou T-C, Wong RJ. Therapeutic inhibition of polo-like kinases in anaplastic thyroid cancer. *Cancer Sci*. 2021;112:803-814. <https://doi.org/10.1111/cas.14769>